Energy & Buildings 332 (2025) 115459

Contents lists available at ScienceDirect

Energy & Buildings

journal homepage: www.elsevier.com/locate/enbuild

Lifetime financial analysis of a model predictive control retrofit for integrated PV-battery systems in commercial buildings

Max Bird [a,*], Reewa Andraos [b], Salvador Acha [a], Nilay Shah [a]

[a] Centre for Process Systems Engineering, Imperial College London, SW7 2AZ, England, United Kingdom
[b] Department of Energy and Environmental Engineering, Institut National des Sciences Appliquées, Lyon, 69100, France

ARTICLE INFO

Keywords:
Model predictive control
Techno-economic analysis
Photovoltaics
Battery storage
Commercial buildings
Load flexibility

ABSTRACT

As electrical grids decarbonise, the need for flexible, real-time energy management systems becomes crucial to handle the variability of renewable sources. This paper investigates the lifetime performance of a commercial PV-battery system under three potential control approaches. Two rule-based controllers and one economic MPC approach are simulated over the lifetime of the battery, considering both the upfront capital and ongoing operational costs. Under the nominal rule-based control, installing the battery system saves 2.9% in operational costs per year. An informed rule-based schedule was then created, based on observing the typical PV and building loads and electricity price dynamics, increasing savings to 4.3%. These additional savings can be realised without any additional capital or operational investment. A supervisory MPC approach is integrated with the existing system control, requiring an upfront investment of $13.7k, combined with additional operational costs of $5.89k/yr. Accounting for these additional costs, net operational savings increase to 6% compared to the baseline operation without a battery system, while also reducing carbon emissions by 9.8%. MPC savings increase to 13.2% when considering the volatile electricity prices seen during the 2022 energy crisis. Despite these encouraging savings, current battery systems remain financially unattractive due to their high upfront cost, and all three control scenarios result in a negative NPV. A sensitivity analysis demonstrates that optimal sizing of batteries and reductions in their cost are the most significant factors when evaluating the lifetime performance of PV-battery systems.

1. Introduction

Countries across the world are looking to decarbonise their electricity networks in line with carbon neutrality goals, reducing their reliance on fossil fuels by installing renewable generation capacity such as wind and solar. However, as renewable energy penetration increases, the temporal mismatch between generation and demand widens. This imbalance can lead to greater energy price volatility and higher levels of generation curtailment [1]. A number of solutions can mitigate these effects, such as international interconnectors [2], grid scale storage solutions [3], demand response services [4] and dynamic spot pricing [5]. The last two of these drive the development of flexible power consumers, who can dynamically alter their load profiles in response to price signals. With buildings responsible for 59% of electricity consumption in the UK [6], they represent a significant source of demand flexibility which can be unlocked through advanced control schemes and enable smart energy systems [7].

Optimal control of building energy systems has been widely researched in the last two decades, covering a range of approaches including fuzzy logic [8], approximate Model Predictive Control (MPC) [9,10] and in recent years notable interest is being shown in Reinforcement Learning (RL) [11,12]. However, the majority of studies use classical MPC approaches due to their intuitive formulation and robust performance [13]. Compared to conventional control approaches which typically track static setpoints, MPC can consider a variety of additional control objectives, including operational cost, energy demand and carbon emissions. Using a combination of predictive system models and short-term data forecasts, MPC optimally schedules the system operation over a receding control horizon subject to user-specified constraints. This forward-looking control approach allows building operators to preempt upcoming disturbances, improving system performance. The increasing number of MPC studies in the built environment has been aided by the ongoing digitalisation of Building Management Systems (BMS) [14]. BMS systems provide two-way communication with assets to col-

* Corresponding author.
E-mail address: max.bird16@imperial.ac.uk (M. Bird).

https://doi.org/10.1016/j.enbuild.2025.115459
Received 13 November 2024; Received in revised form 6 February 2025; Accepted 10 February 2025

Available online 13 February 2025

Nomenclature

Financial Parameters

C_j^{opex}	Total annual operating cost of scenario j
C_{aws}	Total annual cost of Amazon Web Services microservices
$C_{battery}$	Total capital cost of battery system
C_{cloud}^{capex}	Total capital cost to integrate cloud platform with battery system controller
C_{cloud}^{opex}	Total annual operating cost of cloud platform
$C_{elec,api}$	Total annual cost of day-ahead electricity price API
$C_{t,j}^{elec}$	Annual electricity spend for scenario j in year t
e^{ex}	Electricity export price
e_k^{im}	Electricity import price at timestep k
i	Discount rate
O_{bos}	Unit cost of Balance of System for the battery system
$O_{c\&c}$	Unit cost for construction and commissioning of battery system
$O_{irr,api}$	Cost per query of irradiance forecasting API
O_m	Annual unit maintenance cost of battery system
O_{pcs}	Unit cost of Power Conversion System component for the battery system
$O_{storage}$	Unit cost of storage component of battery system
$R_{t,j}$	Net cash inflow of scenario j in year t

Technical Parameters

$\bar{g}$	Average carbon intensity of electricity consumed by the building
ΔT_{ll}	Duration of one low-level control timestep
ΔT_{mpc}	Duration of one MPC timestep
η_c	Charging efficiency of the battery
η_d	Discharging efficiency of the battery
λ	Battery degradation per cycle
C_M	Cumulative battery cycles after M timesteps
E_0^{max}	Initial capacity of the battery
E_M^{max}	Capacity of the battery after M timesteps
E_k	Energy stored in battery at the start of timestep k
G	Annual operational carbon emissions of overall system
g_k	Grid carbon intensity in timestep k
P_k^{bu}	Power demand of the building in timestep k
P_k^{ch}	Power charged to the battery in timestep k
P_k^{dch}	Power discharged from the battery in timestep k
P_k^{ex}	Power exported to the grid in timestep k
P_k^{fixed}	Charging power of battery during fixed charging period
P_k^{im}	Power imported from the grid in timestep k
P_k^{pv}	Power generated by PV in timestep k
P_{max}^{ch}	Maximum charging power of battery
P_{max}^{dch}	Maximum discharging power of battery
P_{max}^{ex}	Maximum grid export limit
P_{max}^{im}	Maximum grid import limit
SoC_{max}	Maximum allowable State of Charge of the battery
SoC_{min}	Minimum allowable State of Charge of the battery
y_k	Binary variable to enforce exclusive charging or discharging of battery within timestep k
z_k	Binary variable to enforce exclusive import or export from the grid within timestep k

lect their operational data, design suitable system models, and deploy control strategies.

Heating Ventilation and Air Conditioning (HVAC) systems are the most commonly considered system in building control studies due to their high energy intensity and worldwide prevalence [15]. The passive thermal mass of the building is used to shift heating loads to the desired periods, while keeping the internal temperature within determined comfort limits. The degree to which a consumer can shift their load can be further increased by incorporating dedicated energy storage technologies, such as Battery Energy Storage Systems (BESS) [16] and thermal storage systems [17]. BESS systems are particularly useful when combined with renewable generation such as rooftop photovoltaic (PV) systems, allowing the building to self-balance its generation and consumption of electricity, but due mostly to their high upfront cost, their real-world deployment is still uncommon. Commercial PV-battery systems typically use rule-based control (RBC), for example maximising self-consumption of on-site generation [18] or a static Time-of-Use (ToU) approach which bases the battery schedule on predetermined electricity price profiles [19].

Simultaneous optimisation of both sizing and operation has also been considered for PV-battery systems. In [20] the optimal battery capacity for a multi-apartment building was considered with a range of possible rule-based control strategies. Findings show that including a battery system does increase the system's self-sufficiency, but even when battery costs are reduced by 50% they are not economically viable. They also note that without significant variability in electricity prices across a day, dynamic price load shifting strategies will perform similarly to existing rule-based controllers. Similar work is presented for optimising a PV-battery system in a 3-story office building in China [21]. Results show that optimising the rule-based control based on peak-valley electricity pricing can reduce battery cycle ageing by 63.5%, while reducing LCOE by 14%. The larger savings are due to the lower capital cost of the battery, and a high peak-to-base ratio of 3 for the electricity prices. Overall, in recent academic literature MPC solutions are becoming popular for these systems, as their predictive nature can unlock additional savings through improved short-term scheduling.

In [22] an interesting combination of predictive and rule-based control is considered for a commercial PV-BES system in an educational institute. Firstly, predictive models forecast the day-ahead building load and PV generation, which is used to inform the rule-based battery controller which aims to minimise the peak power consumed from the electrical grid. The formulated objective function is nonlinear and as such is solved using a Genetic Algorithm (GA) approach. Installing the PV-BES system with this controller is shown to reduce the building's energy cost by up to 37% compared to a baseline without the PV-BES system installed. Additionally, savings are shown to be strongly seasonally dependent, providing the biggest improvement in Spring and the smallest improvement in Autumn. As highlighted by the authors, future work in this area needs to evaluate the end-to-end financial benefit of implementing the PV-BES and its control system, including the initial investment and operational costs.

In [23] authors present a real-world deployment of an MPC scheme for a commercial building in the USA with PV and battery systems. They quantify the ability of the building to provide demand flexibility (DF) services or Time of Use (ToU) optimisation considering HVAC, refrigeration and battery systems. They also describe the open-source hardware/software infrastructure required to deploy the MPC scheme in the building, however the setup and operational costs are not included in the financial analysis. Results show that the MPC scheme was able to provide a range of DF services including load shifting and load shedding; the long term operation of the controller over 1 year led to a 12% cost saving while respecting thermal comfort and food safety.

A real-world cloud-based deployment of model predictive control for a commercial battery system is presented in [24]. The controller is deployed for a 150 kWh lithium-ion battery at an office of 100+ staff, polling the battery controllers and electricity submeters and extracting data into the cloud at 1 to 10 minute frequency using a bi-directional MQTT connection. A range of interesting implementation issues are discussed, mostly related to data outages due to equipment failure and IT errors. Despite the rich discussion around implementing the solution, there is no discussion of the additional costs required to deploy the MPC scheme. This could be due to the authors finding that the 5.5% electricity bill reduction was no sufficient to payback even the battery system alone over its lifetime.

The optimal management of a residential PV-battery system, considering grid scheduled blackouts and battery lifetime, is presented in [25]. Their economic MPC formulation considers both the operational and lifetime cost of the battery system, while ensuring the building load is always satisfied. The simulated case study evaluates the seasonal performance of the MPC scheme across a range of scenarios, assuming perfect prediction models for the building/PV loads and the grid blackout schedule in all cases. When explicitly considering loss in battery capacity due to battery schedule in the objective function, the overall cost to supply the home increases by around 5-10%, however this does not include any capital or operational costs to deploy the MPC scheme.

In this paper, the lifetime performance of a commercial PV-battery system is simulated under three control scenarios, two rule-based controllers and a perfect prediction MPC model, to identify the performance gap between existing and state-of-the-art control approaches. Simulations are based on real-world data gathered from a commercial PV-battery installation in the UK. This work builds upon our existing experience deploying MPC control retrofits for HVAC systems [26], expanding our modelling and control frameworks to other systems in the built environment. As discussed above, the existing literature on MPC deployments often neglects the additional costs required to deploy and maintain these advanced control solutions. This both reduces the uptake of such retrofits, as their financial requirements are unclear, and inflate their expected savings. As a result, the major contributions of this study include:

- Quantifying the lifetime financial performance of each control approach, taking into account the additional capital and operational costs associated with a real-world MPC deployment. This point is particularly lacking in the current literature.
- A detailed sensitivity analysis of key parameters to understand the performance of each control approach under a range of market conditions, highlighting the economic gap to make such solutions competitive.

Overall, this analysis will inform both academics and building industry experts, hence bridging the gap between theoretical studies and implementable MPC solutions. The paper is organised as follows: Section 2 formulates the system modelling and control methodology, Section 3 outlines the case study and control scenarios considered, Section 4 presents the performance of each scenario including a sensitivity analysis, Section 5 discusses the results before concluding the main findings in Section 6.

2. Methodology

This paper presents a lifetime financial analysis for three control schemes for a grid connected PV-battery system, outlined in more detail in Section 3. In this section the mathematical representation of the system is introduced, followed by a summary of the different control approaches. In each case, the controller is responsible for managing the power flows of the battery system (charge/discharge) and the grid connection (import/export) in order to supply the required building load at each timestep, while accounting for on-site generation from the installed PV system.

2.1. System models

In order to assess the lifetime performance of each control scheme, a basic model of the system is developed based on the system configuration described in Section 3. An overall energy balance of the system is outlined in Equation (1),

$$P_k^{im} + P_k^{pv} + P_k^{dch} = P_k^{ex} + P_k^{bu} + P_k^{ch} \tag{1}$$

where P_k^{im} is the power imported from the grid, P_k^{PV} is the power generated from onsite PV, P_k^{dch} is the power discharged from the battery, P_k^{ex} the power exported to the grid, P_k^{bu} is the building load, P_k^{ch} is charging rate of the battery system and k is the discrete timestep. Here grid and battery power flows are separated into their import/export and charge/discharge components to account time-varying electricity prices as explained in later sections. The battery storage model is outlined in Equation (2),

$$E_{k+1} = E_k + \left[\eta_c P_k^{ch} - \frac{1}{\eta_d} P_k^{dch}\right] \Delta T \tag{2}$$

where E_k is the energy stored in the battery at timestep k, and ΔT is the duration of one timestep. As discussed in [27] battery degradation mechanisms are varied and complex, affected by a range of factors including the number of cycles, the State of Charge (SoC), the Depth of Discharge (DoD), the cell temperature and the elapsed time. For example, authors in [28] apply a physics-based reduced-order battery degradation model from [29] to an ageing aware battery control approach. The resulting cumulative capacity fade was shown to be roughly a linear function of the battery cycling, and hence in this paper a simple linear degradation in battery capacity is assumed as expressed in Equations (3) - (4),

$$E_M^{max} = E_0^{max} \left[1 - C_M \lambda\right] \tag{3}$$

$$C_M = \sum_{k=0}^{M} \frac{|E_{k+1} - E_k|}{2E_0^{max}} \tag{4}$$

where E_0^{max} is the initial capacity of the battery, E_M^{max} is the capacity of the battery after M timesteps, C_M is the cumulative number of full battery cycles after M timesteps and λ is the degradation of the battery storage per full cycle of the battery, expressed in [%/cycle]. In all scenario simulations the battery capacity E_M^{max} is updated every week using Equation (3).

2.2. Rule-based control

The installation has an existing rule-based controller for the BESS as depicted in the bottom of Fig. 2. At each control timestep, the rule-based control can operate in 2 distinct sub-modes: (1) fixed charge and (2) self-consumption mode. The time windows for each sub-mode are defined in a daily schedule, summarised later in Fig. 4. In the fixed charge mode the battery is charged at a constant power, P_k^{fixed}, chosen by the user. The self-consumption mode aims to eliminate any grid import or export depending on the measured building and PV load. If the current PV load is greater than the building load, the controller will charge the battery with the excess PV generation. On the other hand if the building load is greater than the PV load, the battery will discharge to supply the deficit. The rule-based controller is also subject to the battery power and storage level constraints in Equations (6), (7) and (10). If these constraints become active the grid will be used for the remainder, for example if the battery is at its upper SoC limit any additional excess PV will be exported, and if the battery is at its lower SoC limit, any power deficit will be imported. A flowsheet of the overall logic for the rule-based control is shown in Fig. 1.

2.3. MPC formulation

In the proposed strategy, the MPC formulation minimises the overall electricity spend over the forecast horizon N, taking into account separate import costs and export earnings, as shown in Equation (5),

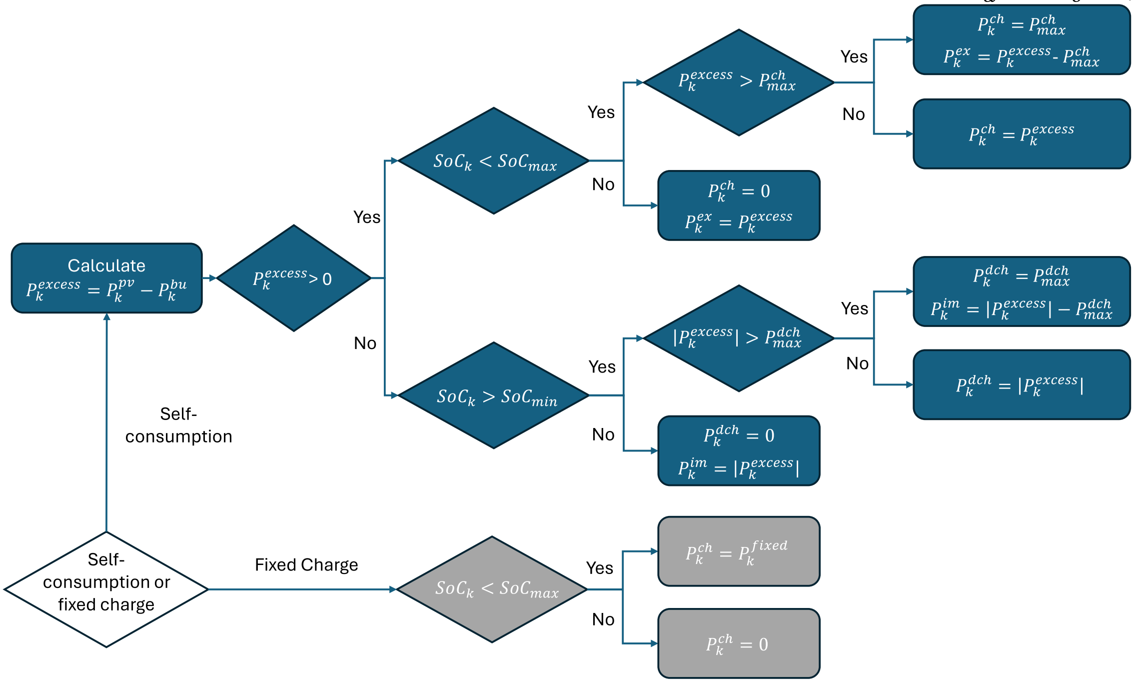

Fig. 1. Flowsheet demonstrating logic for rule-based control which is run at every low-level control timestep.

$$J = \min_{P_k^{im}, P_k^{ex}} \sum_{k=0}^{N} \left[e_k^{im} P_k^{im} - e^{ex} P_k^{ex} \right] \Delta T_{mpc} \tag{5}$$

where e_k^{im} is the time-varying electricity purchase price, e^{ex} is a fixed export price, and ΔT_{mpc} is the timestep of the MPC scheme. Equations (1) and (2) are re-used to enforce the overall energy balance of the system, and are formulated as constraints in the optimisation, along with the physical system constraints listed below:

$$0 \le P_k^{ch} \le y_k P_{max}^{ch} \tag{6}$$

$$0 \le P_k^{dch} \le \left[1 - y_k\right] P_{max}^{dch} \tag{7}$$

$$0 \le P_k^{im} \le z_k P_{max}^{im} \tag{8}$$

$$0 \le P_k^{ex} \le \left[1 - z_k\right] P_{max}^{ex} \tag{9}$$

These constraints limit the charging and discharging rates of the battery, and the import and export limits for the grid. Binary variables y_k and z_k are used to enforce exclusive charging or discharging of the battery and exclusive import or export from the grid within one timestep. As the battery functions primarily to provide backup power in the case of a power cut, a lower SoC limit is set to ensure there is always a minimum quantity of energy in storage. To prevent losses and increased self-discharge the upper SoC limit of the battery is also set. These constraints are shown in Equation (10). The minimum SoC is related to the starting capacity of the battery as the reserve energy should not decrease as the battery capacity degrades. The upper SoC limit however will change as the battery capacity degrades and so the point-in-time capacity is used.

$$SoC_{min} E_0^{max} \le E_k \le SoC_{max} E_M^{max} \tag{10}$$

Fig. 2 gives an overview of how the existing low-level control works, and how it interacts with the supervisory MPC scheme. The MPC controller operates at a longer timestep than the existing system control, providing a setpoint to the battery controller, $P_{battery}^{mpc}$, which is held constant over the MPC timestep, ΔT_{mpc}. In reality the building and PV loads will be changing throughout the MPC timestep, and so the existing battery controller ensures that the overall energy balance, Equation (1), is adhered to at every low-level timestep, ΔT_{ll} by changing the grid import/export.

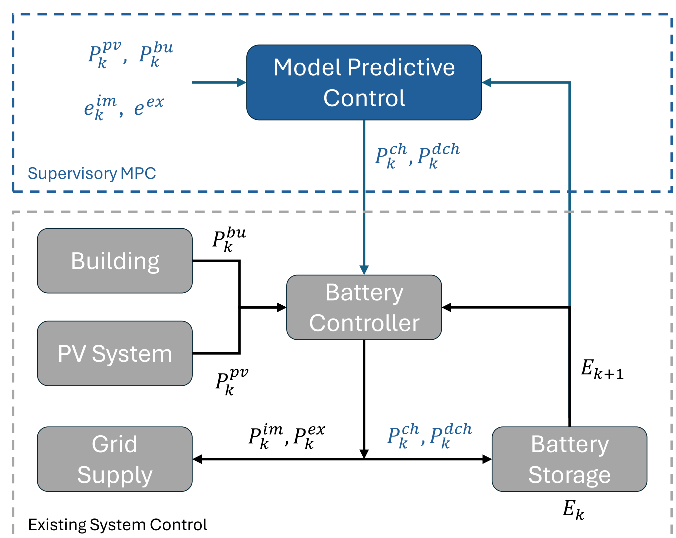

Fig. 2. Supervisory MPC integration with existing system control.

3. Case study

3.1. System description

This study is based on a commercial, grid-connected PV-battery system in a UK supermarket, as depicted in Fig. 3. A 300 kWp photovoltaic (PV) array is fitted to the roof, using a set of DC/AC inverters to supply a 3-phase, 400V AC bus which is connected to the grid supply point, building incomer and battery system. Due to network constraints from the Distribution Network Operator (DNO), the grid import capacity of the site is limited to 250 kVA. In addition the export capacity is limited to 250 kVA under a G99 connection and, assuming the transformer has

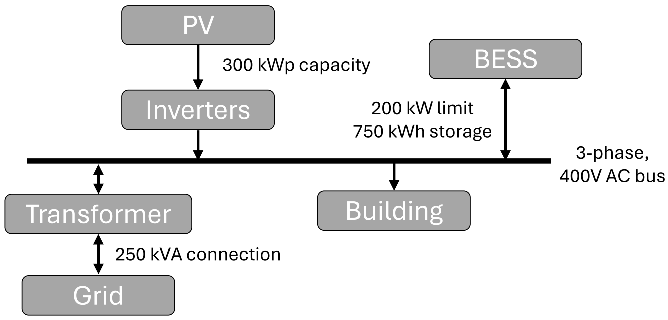

Fig. 3. System configuration.

Table 1
Summary of technical parameters, battery degradation calculated from [30] and battery efficiencies taken from [31].

Parameter	Symbol	Unit	Value
Minimum SoC Limit	SoC_{min}	%	40
Maximum SoC Limit	SoC_{max}	%	95
Installed Battery Capacity	E_0^{max}	kWh	750
Battery Power Limits	P_{max}^{dch}, P_{max}^{ch}	kW	200
Battery Efficiencies	η_c, η_d	%	94
Grid Power Limits	P_{max}^{ex}, P_{max}^{im}	kW	237
Battery Degradation	λ	%/cycle	0.0096
MPC Timestep	ΔT_{mpc}	min	30
Low-Level Timestep	ΔT_{ll}	min	5

a power factor of 0.95, this gives an effective import/export limit of 237 kW.

To ensure the building's critical systems can be powered in the event of a power cut, a Battery Energy Storage System (BESS) was installed. It uses 750 kWh Lithium Nickel Manganese Cobalt (NMC) cells, with a rated AC charge/discharge up to 200 kW. Typically in supermarkets this emergency power functionality is provided by a backup diesel generator, but here a battery system was chosen for two main reasons: (1) to provide peak shaving if grid import limits are breached (2) better utilise the on-site PV generation to reduce the overall carbon emissions of the site. To ensure this backup supply is always available, the lower SoC limit is 40% and to maintain good battery health the upper SoC limit is 95%. The degradation of battery storage is based on the manufacturer warranty, which guarantees a 3.5% degradation rate per year, based on one full charge/discharge cycle per day [30]. The technical specifications of the system are summarised in Table 1.

One year of historical energy datasets were collected from the site, covering the period from July 2023 - July 2024. Pulse meters log the cumulative energy flow for each system every 5 minutes, allowing us to calculate the average power flows over each interval. The storage level of the battery is also logged at the same interval. Hourly, wholesale, day-ahead electricity prices for the UK were collected from NordPool [32], and combined with other relevant network and environmental obligation charges as outlined in [33], to generate the site's electricity price profile. National Grid ESO provides an API service to quantify the historical carbon intensity of the grid, based on the generation mix at half-hourly resolution [34].

3.2. Scenarios

The scenarios considered in this study are outlined in Table 2. In addition to the three control scenarios, a baseline scenario is introduced where the building has a grid connection and onsite PV, but no BESS installed. This acts only as a reference scenario to calculate the savings of the three proposed control scenarios. S1 represents the nominal rule-based control approach used in the system. From 00:00 - 06:00, a fixed charge occurs to fully charge the battery, utilising cheap electricity prices during the early hours of the day. From 06:00 - 00:00 the

Table 2
Overview of scenarios considered.

Scenario	Battery Control	Systems Considered			
		Grid	PV	BESS	Cloud
Baseline	None	x	x		
S1	Rule-based	x	x	x	
S2	Rule-based	x	x	x	
MPC	Model Predictive Control	x	x	x	x

system operates under a self-consumption mode as described in Section 2.2. This maximises on-site consumption of PV generation to reduce the site's electricity spend and carbon emissions. However, during initial studies of this control approach some areas for improvement were identified. First, the length of the morning charge period meant that during the self-consumption period the battery would reach the upper SoC limit relatively early in the day, leading to significant export of excess PV generation. Secondly, the second half of the self-consumption period, when the building load is supplied by the battery system, did not always coincide with the high electricity price period taking place from 17:00 - 19:00.

S2 was introduced to use the same rule based control logic, but better schedule the charge and self-consumption periods by analysing the typical building load and daily electricity price patterns. In this scenario, the initial fixed charge period is reduced to 00:00 - 04:00, followed by a four hour self-consumption period from 05:00 - 09:00. During this self-consumption period the battery charge limits are set to [-200,0], meaning the battery can only discharge. As a reminder, during this self-consumption mode, the battery will only discharge power equal to the current building demand. This provides a small arbitrage opportunity, while also ensuring the battery is at its lower storage limit as the sun starts to rise to allow as much excess PV generation as possible to be stored in the battery system for the next self-consumption period from 09:00 - 17:00. During this next period the battery is not allowed to discharge. The final self-consumption period is from 17:00 - 00:00 and here the battery is allowed to discharge to align with the aforementioned evening spike in electricity price. Both schedules for S1 and S2 are outlined in Fig. 4.

The third scenario uses the supervisory MPC approach outlined in Section 2.3. The MPC timestep was chosen as 30 minutes, and a forecast horizon of 12 hours was chosen to align with availability of day-ahead electricity prices. Perfect prediction models for both the PV generation and building load are used, wherein the MPC is provided the measured average power flows across each MPC timestep for the entire forecast horizon. This assumption allows us to quantify the best possible performance of a supervisory MPC scheme in this type of application, and can easily be modified in future work using predictive building load [35] and PV generation models [36] available in literature. The MPC scheme is considered to be deployed in a cloud-based platform as demonstrated in our previous work [26].

3.3. Lifetime financial analysis

To quantify the relative financial performance of each control approach, the three scenarios are simulated over the lifetime of the system, defined as the time until the BESS degrades to 70% of its starting capacity. By defining the lifetime in this way, it captures any trade-offs in aggressive strategies which may have greater initial cost savings, but result in premature degradation of the battery. To facilitate this, the one year of historical data is extrapolated into the future using a number of assumptions. PV generation capacity is assumed to degrade linearly at a rate of 0.98%/yr, as presented in [37] which studied the degradation of similar sites in the UK and grid carbon intensity is assumed to reduce by 7.5% year-on-year, inline with the historical decarbonisation rate observed from 2019 - 2024 [34].

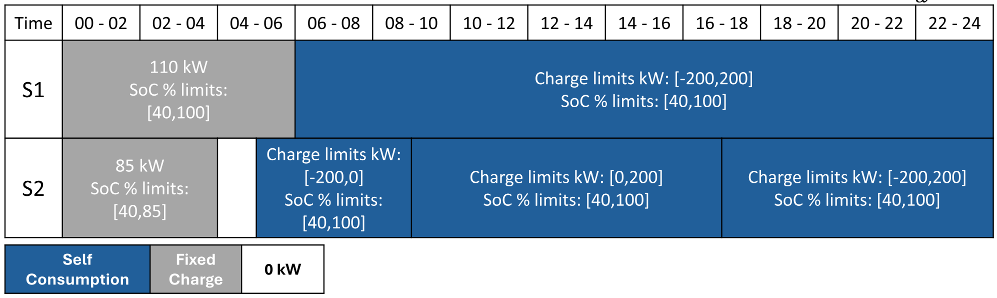

Fig. 4. Overview of the daily BESS charging schedule for scenarios S1 and S2.

The Net Present Value (NPV) of a project is typically used to quantify the financial attractiveness of an investment. It calculates the current value of a future stream of annual payments from a project, taking into account the upfront capital expenditure (CAPEX) and ongoing operating expenditure (OPEX), shown in Equation (11).

$$NPV = \sum_{t=0}^{N} \frac{R_t}{(1+i)^t} \tag{11}$$

where R_t represents the net cash inflow during year t and i represents the discount rate, which is the expected rate of return from a similar project. The overall capital cost of the battery system, $C_{battery}$, is shown in Equation (13) using the approach presented in [38], which breaks the BESS cost into four components: (1) energy storage, $O_{storage}$, (2) Power Conversion System (PCS), O_{pcs}, (3) Balance of System (BOS), O_{bos}, and (4) Construction and Commissioning (C&C), $O_{c\&c}$. The MPC scenario includes an additional capital cost to integrate the existing battery control system with the cloud-based platform, C^{capex}_{cloud}. This cost was quoted from a 3rd party provider, and includes connecting and configuring a Modbus connection from the battery controller to an existing gateway device in the store, which connects to the cloud platform via an Ethernet connection. The total CAPEX for the MPC scenario is assigned as a negative cashflow in year 0, as shown in Equation (12). S1 and S2 require no integration with the cloud and so this term is not included for these scenarios.

$$R_0 = -C_{battery} - C^{capex}_{cloud} \tag{12}$$

$$C_{battery} = \left(O_{storage} + O_{c\&c}\right) E^{max}_0 - \left(O_{pcs} + O_{bos}\right) P^{ch}_{max} \tag{13}$$

The subsequent annual cashflows, $R_{t,j}$, for each scenario, j are calculated using Equation (14). This is the difference in electricity spend between the scenario $C^{elec}_{t,j}$, and the baseline case, $C^{elec}_{t,baseline}$, accounting for any ongoing operating costs, C^{opex}_j. The annual electricity cost for each scenario is shown in Equation (15), using the site specific variable import price, e^{im}_k, and fixed export price, e^{ex}.

$$R_{t,j} = C^{elec}_{t,baseline} - C^{elec}_{t,j} - C^{opex}_j \tag{14}$$

$$C^{elec}_{t,j} = \sum_{k=0}^{T} \left[e^{im}_k P^{im}_{k,j} - e^{ex} P^{ex}_{k,j} \right] \tag{15}$$

All three control scenarios have an ongoing operating cost relating to the maintenance of the battery system. In addition, the MPC scenario includes the operating cost for the cloud-based platform. The overall operating cost for each scenario is shown in Equation (16). The MPC cloud costs are composed of the cloud infrastructure costs to host the data storage and control logic in Amazon Web Services (AWS), C_{aws}, as well as an annual membership for the day-ahead electricity price API from NordPool, $C_{elec,api}$ and irradiance forecasting API from OpenWeather, $O_{irr,api}$. Although this approach uses a perfect prediction MPC model, and as such not using forecasts of irradiance, this cost would be required in a real MPC deployment, and so it is included in our analysis. All input parameters are summarised and referenced in Table 3. Note that electricity prices and cloud CAPEX and OPEX costs were converted from GBP to USD, using an exchange rate of 1.30 USD per GBP.

Table 3
Summary of financial parameters, [a] was quoted from a third party provider while [b] were provided by the building operator.

Parameter	Symbol	Unit	Value	Ref
Storage Capital Cost	$O_{storage}$	$/kWh	161	[39]
PCS Capital Cost	O_{PCS}	$/kW	184	[38]
BOS Capital Cost	O_{BOS}	$/kW	97	[38]
C&C Cost	$O_{c\&c}$	$/kWh	98	[38]
Maintenance Cost	O_m	$/kW/yr	8	[38]
Cloud Capital Cost	C^{capex}_{cloud}	$k	13.7[a]	-
Cloud AWS Infrastructure	C_{aws}	$/yr	163	[26]
Electricity Price API	$C_{elec,api}$	$k/yr	1.88	[32]
Irradiance Forecasting API	$O_{irr,api}$	$/request	0.13	[40]
Electricity Export Price	e^{ex}	$/kWh	0.08[b]	-
Discount Rate	i	%	10[b]	-
Grid Decarbonisation	-	%/yr	7.5	[34]
PV Degradation	-	%/yr	0.96	[37]

$$C^{opex}_j = O_m P^{ch}_{max} + C^{opex}_{cloud} \tag{16}$$

$$C^{opex}_{cloud} = C_{aws} + C_{elec,api} + O_{irr,api} \frac{60(24)(365)}{\Delta T_{mpc}} \tag{17}$$

In addition to the financial metrics, the total carbon emissions and average carbon intensity of each scenario are also presented. In the UK, the half-hourly carbon emissions of the grid, g^{grid}_k, are calculated by National Grid, and made available through their carbon intensity API [34]. Using these data, along with the simulated grid import power in each scenario, P^{im}_k, the annual carbon emissions G can be calculated from Equation (18),

$$G = \frac{\Delta T_{ll}}{60} \sum_{k=0}^{N} P^{im}_k g_k \tag{18}$$

where N is the total number of low-level timesteps in a year. This calculation assumes onsite PV generation has no associated carbon emissions. The average carbon intensity of electricity consumed by the building, $\bar{g}$, can then be calculated using Equation (19).

$$\bar{g} = \frac{60G}{\Delta T_{ll} \sum_{k=0}^{N} P^{bu}_k} \tag{19}$$

4. Results

First a comparison of the annual performance of each scenario is presented, followed by a summary of the lifetime financial performance. Finally a sensitivity analysis is conducted on key parameters to understand the performance of the MPC solution under different conditions.

4.1. Annual performance

Fig. 5 shows the daily performance of each control scenario for a summer day. From the plot it is clear that S2 is performing as expected,

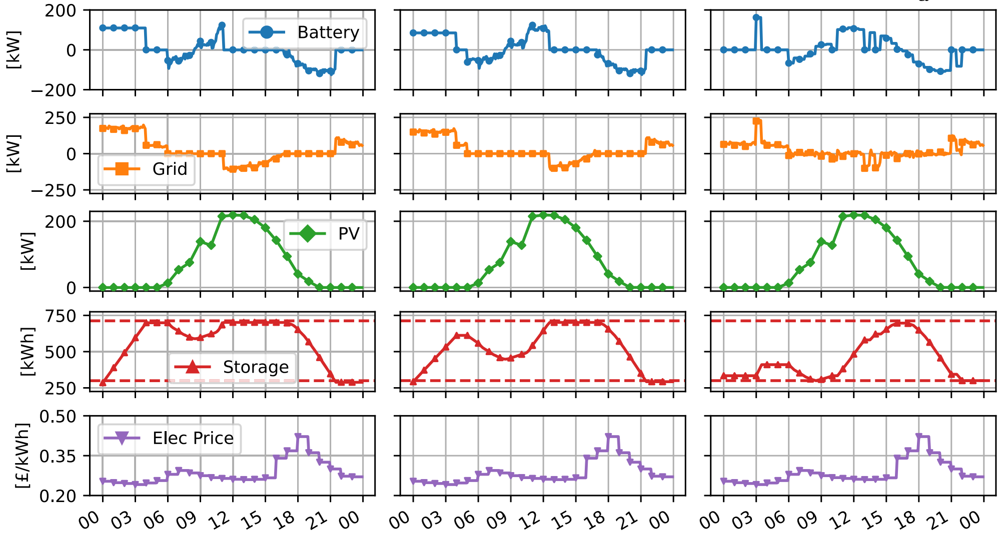

Fig. 5. Daily plot of S1 (left), S2 (middle) and MPC (right) for an August day.

improving the utilisation of on site PV generation compared to S1. S2 both reduces the morning fixed charge period to 4 hours, and starts discharging the battery one hour earlier, allowing the battery to store more of the excess PV generation from 09:00 - 13:00. This in turn leads to a reduction in exports from the site which is favourable as the fixed export price of 0.08 $/kWh is lower than the lowest import price of around 0.29 $/kWh. The MPC further improves the performance compared to S2 via the same mechanism. Due to its 12 hour forecast horizon the MPC controller can pre-empt the large volume of PV generation that will occur during the day, and hence decides to only charge a very small amount in the morning from 03:00 - 04:00. This leaves the entire usable capacity of the battery free to store excess PV generation from 09:00 - 16:00.

Fig. 6 shows the daily performance of each scenario for a day with lower PV generation in January. In this situation the building load will almost entirely consume the onsite PV as it is generated, and so the control system should ideally focus on price arbitrage. Here S2 actually performs worse than S1 as its scheduling is optimised for days with excess PV generation, which is more impactful for the annual performance. During winter days the earlier self-consumption discharge period in S2 from 05:00 - 09:00 isn't needed as all PV is immediately consumed by the building. Ideally the battery controller could use different rule-based strategies depending on the season, however this would require recommissioning the controller throughout the year. These engineering service costs would be high and exceed the potential savings. In the MPC scenario there are two clear load shifting events, first a small charging event at 02:00 and discharging from 06:00 - 10:00, then a larger charging event from 14:00 - 16:00 allowing it to fully discharge the usable battery capacity from 17:00 - 22:00 during the high price period, reducing grid imports as much as possible.

Table 4 summarises some key performance indicators (KPIs) for the first year of operation to contextualise the relative performance of each control scenario compared to the baseline. As discussed, all scenarios lead to an increase in direct PV utilisation, shown by the decreasing export volumes, from 68 MWh in the baseline to 25 MWh for the MPC scenario. Due to load shifting behaviour, all control scenarios actually result in a greater net volume of electricity imports compared to the baseline case. For example, S1 imported 509 MWh net compared to only 488 MWh in the baseline, however as expected the net import cost is lower, as overall the electricity is imported at a lower price. The MPC scenario for example reduces net import costs by $16.6k compared to the baseline and $9.9k compared to S1, a 9.6% and 6.0% saving respectively. Compared to the baseline, all control scenarios reduce operational carbon emissions, even though these are not explicitly considered in any of the control scenarios. Day-ahead electricity prices are high during periods of high demand, which is generally when more carbon intensive generation sources are powering the grid. As our control scenarios aim to reduce consumption during high-price periods, this also indirectly reduces the average carbon intensity of electricity consumed on site. The MPC scenario reduced annual carbon emissions to 71.5 tCO_2, a reduction of 9.8% compared to the baseline, and 4.6% compared to S1.

Table 4
Annual electricity volumes/costs for imports and exports, and annual carbon emissions and average carbon intensity in Year 1.

KPI	Baseline	S1	S2	MPC
Electricity Import [MWh]	555	552	534	530
Electricity Export [MWh]	68	43	27	25
Net Import [MWh]	488	509	507	505
Electricity Import [$k]	178	169	165	158
Electricity Export [$k]	5.3	3.4	2.1	2.0
Net Import [$k]	173	166	163	156
CO_2 Emissions [tCO_2]	79.3	74.9	73.7	71.5
CO_2 Intensity [gCO_2/kWh]	95.9	90.6	89.2	86.5

4.2. Lifetime financial analysis

The breakdown of CAPEX and OPEX for each scenario is shown in Fig. 7. S1 and S2 both use the existing rule-based control framework, and so have the same CAPEX and OPEX costs totalling $250k and $1.6k/yr respectively. For the MPC deployment an additional $13.7k is required to integrate the battery controller with the cloud-based platform, bringing the total CAPEX for this scenario to $263.7k. The $250k battery cost is split into $120k (48%) for the storage packs, $73.5k (28%) for the construction and commissioning, $36.8k (15%) for the power control system and $19.4k (9%) for the balance of system. This brings the total unit storage cost to $333/kWh. In addition to the ongoing battery maintenance, the operating costs for the MPC scenario include an annual subscription to the NordPool API for day-ahead electricity prices $1.85k/yr, use of the irradiance forecast API $2.28k/yr, and ongoing platform costs for AWS $0.16k/yr. This brings the overall operating cost for the MPC scenario to $5.89k/yr.

Table 5 summarises the lifetime performance of each scenario with reference to the baseline case. As discussed, S2 benefits from the informed rule-based scheduling, increasing the net savings in year 1 from $5.1k in S1 to $7.6k. Interestingly, S2 also utilises the battery storage slightly less than S1, only cycling 750 kWh/day compared to 823 kWh/day in S1. This leads to a notable increase in the battery lifetime, from 15.6 years to 17.1 years. The MPC scenario also provides an im-

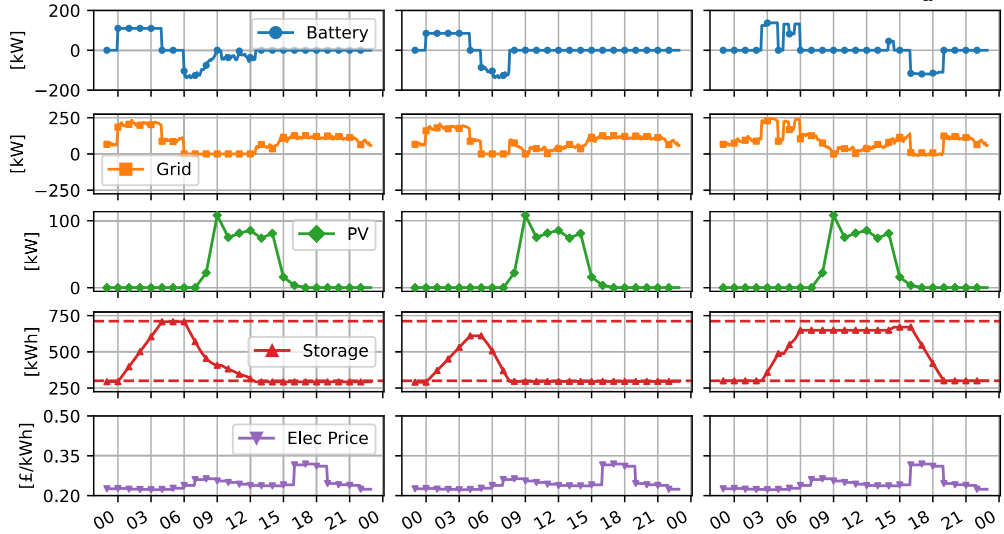

Fig. 6. Daily plot of S1 (left), S2 (middle) and MPC (right) for a January day.

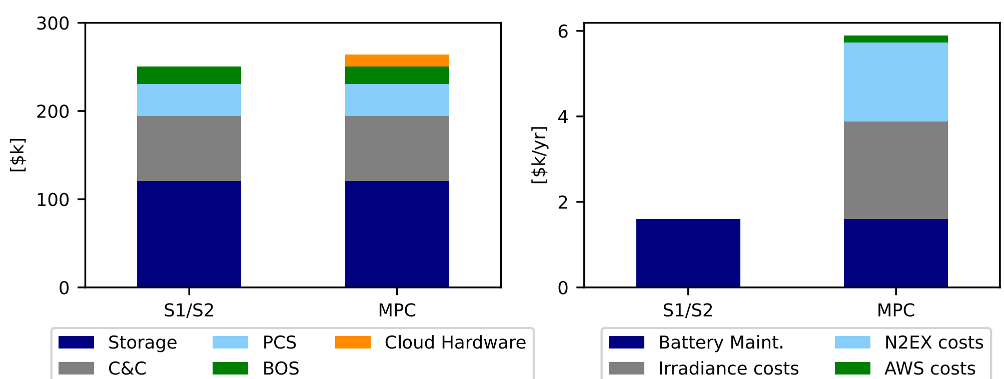

Fig. 7. CAPEX OPEX breakdown.

provement compared to S2 and, taking into account the $5.89k/yr OPEX costs, the net savings in year 1 increase from $5.1k in S1 to $10.7k in the MPC case. Interestingly the battery lifetime is again increased to 20.3 years by utilising the battery less, only cycling 635 kWh/day on average. For each scenario, the battery lifetime is defined as the time to reach 70% of original storage capacity, which in these simulations took 3,100 cycles. These estimated battery lifetimes are higher than those quoted in other studies which typically quote lifetimes of 10 years with 2,000+ cycles [41]. This is primarily due to selecting a 70% capacity degradation as end of life, rather than the industry standard 80% threshold. By choosing a lower capacity threshold the lifetime utilisation of the expensive BESS is increased therefore increasing its capital recovery.

Notably in all scenarios the NPV is negative, meaning that installing the battery system under any control approach is not financially attractive. This result is due to two main causes; the high unit storage cost of current NMC battery cells, and the fact that the lower SoC is limited to 40% in order to provide backup supply and peak shaving to the store. In this sense the NPV for each scenario could be interpreted as the lifetime cost to provide this backup power functionality using a battery system. It is worth noting that no residual value is assigned to the battery but in future, as the second-hand battery market develops, it could be sold on. In any case, there is a clear improvement in NPV across each scenario, from -$213k in S1, to -$195k in S2, to -$187k for MPC.

Table 5
Summary of lifetime KPIs for nominal price scenarios.

Lifetime KPIs	S1	S2	MPC
CAPEX [$k]	250	250	264
OPEX [$k/yr]	1.60	1.60	5.89
Year 1 Net Savings [$k]	5.1	7.6	10.7
NPV [£k]	-213	-195	-187
IRR [%]	-14.2	-9.8	-6.5
Battery Lifetime [yr]	15.6	17.1	20.3
Battery Usage [kWh/day]	823	750	635

4.3. Sensitivity analysis

This section presents a sensitivity analysis of a number of variables to better understand how the NPV of the MPC solution varies under a range of conditions. Firstly the total CAPEX of the battery system is varied, to inform future deployments when battery costs are expected to reduce [42], and on the other hand for operators who may only have access to more expensive systems. The cloud operating costs are also included for the same reasons. Electricity price and discount rate are also both studied, to inform a wider range of users who may have access to different prices and discount rates in different regions. Finally the installed battery capacity is varied, to inform users who are yet to install a battery system.

Fig. 8 shows the effect on lifetime NPV for the nominal MPC case with corresponding percentage changes in key financial parameters. The

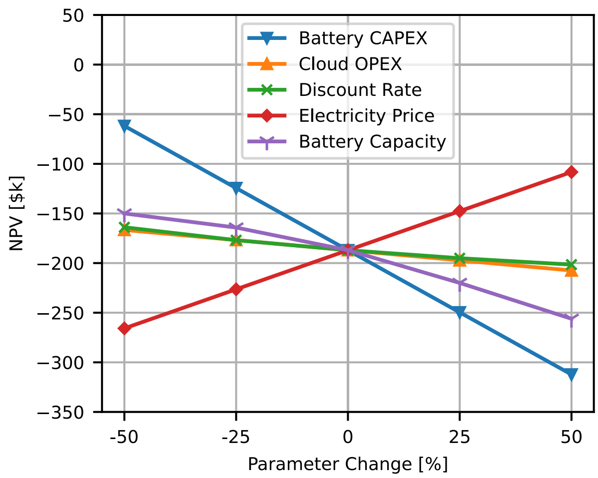

Fig. 8. Sensitivity analysis for nominal MPC formulation.

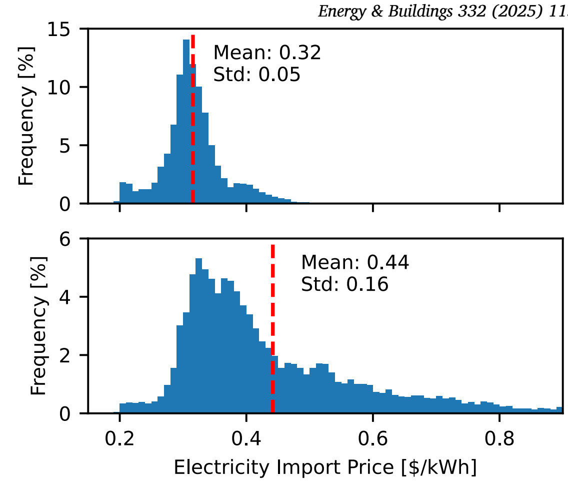

Fig. 9. Histogram for annual electricity prices for the nominal prices, July 23' - July 24' (top) and the high volatility prices, July 22' - July 23' (bottom).

battery cost is the most sensitive parameter, with a 50% reduction in total battery cost resulting in an increase in NPV from -$187k to -$62k. Extrapolating this trend further, the total battery capital cost would need to decrease by 75% in order to reach an NPV of 0, equating to a total unit storage cost of $83/kWh. At this point the savings from MPC operation of the battery system would completely offset its cost, essentially providing the backup power functionality for free. As expected the electricity price is also an impactful variable, increasing the NPV from -$187k to -$108k when prices are increased by 50%. The cloud operating costs and discount rate are less impactful. The battery capacity sensitivity shows that the storage size could have been decreased by 50% to increase NPV from -$187k to -$149k, however this would also reduce PV utilisation and increase overall carbon emissions.

The sensitivity analysis presented in Fig. 8 demonstrates the effect of linearly scaling each variable in question. When considering the effect of electricity price on the MPC performance, it is not only the magnitude of the electricity price which matters, but also the variation in price across a day. For example, in days with greater variation in electricity price (higher volatility) the effect of load shifting should be much more significant as the difference between the high and low prices increases. To investigate this, a high price volatility scenario was considered using day-ahead electricity prices from July 2022 - July 2023 instead of the nominal July 2023 - July 2024 prices. These higher volatility prices were a result of the Russian invasion of Ukraine in 2022. This more volatile day-ahead price profile could also represent electricity prices in the future, where renewable penetration onto the grid is high. Fig. 9 compares the distribution of electricity prices in these two cases. In the nominal case, the electricity price has a low volatility with a standard deviation of just 0.05 $/kWh; in the high volatility case this increases by more than a factor of 3 to 0.16 $/kWh. The mean price also increases from 0.32 $/kWh to 0.44 $/kWh.

Under this scenario of increased price volatility, the MPC scheme performs much better, as shown in Table 6. The net savings in year 1 increase by over a factor of 2, from $10.7k to $22.8k. NPV is similarly improved, going from -$187k to -$99k. The battery utilisation is also higher, due to the more favourable load shifting conditions, increasing from 635 kWh/day in the nominal price case to 731 kWh/day in the volatile price case. This has a knock on effect on the battery life, which is decreased from 20.3 to 17.6 years.

Table 6
Summary of lifetime KPIs for nominal and volatile price cases.

Lifetime KPIs	MPC - Nominal Prices	MPC - Volatile Prices
Year 1 Net Savings [$k]	10.7	22.8
NPV [£k]	-187	-99
IRR [%]	-6.5	1.3
Battery Lifetime [yr]	20.3	17.6
Battery Usage [kWh/day]	635	731

5. Discussion

The existing rule-based controller presented in S1 is notably improved in both S2 and MPC scenarios via two main mechanisms: (1) improving onsite PV utilisation, (2) improved load shifting considering time-varying import prices. S2 uses the same rule-based control logic as S1, but with an updated schedule that takes into account general patterns in the building load, PV generation and electricity price dynamics. In the first year of operation S2 saved $7.6k net relative to the baseline scenario, compared to $5.1k in S1, an increase of 49%. These savings are easy to obtain without any capital or operational investment, and should be considered for all existing PV-battery installations. The perfect MPC scenario further reduces electricity cost, saving $10.7k net compared to the baseline and increasing savings by 110% compared to the nominal rule-based control in S1. However it is important to note that this formulation uses perfect predictions of building and PV loads, and as such it represents the best-case performance of an MPC solution. This should be addressed in future work by considering forecast uncertainty and implementing predictive building load and PV generation models.

This work clearly highlights the importance of considering implementation costs for MPC approaches. If only the operational savings are considered, the performance of the MPC solution can be overestimated. For example, the MPC scenario saved $16.3k in electricity cost in year 1 compared to the baseline, however this requires ongoing operational overhead of $5.89k/yr, reducing the potential savings by nearly 35%. Over 96% of the MPC operating costs are related to using the electricity price and irradiance forecasting APIs, and this could represent an easy area to cut costs in other use-cases. For example, if the user knows their electricity price profile in advance, or they can estimate their PV generation based on freely available weather forecasts. Alternatively, if a system operator has multiple installations these costs can be split across each location. In addition to the extra operating costs, an upfront cost of $13.7k is required to integrate the cloud-based MPC solution onsite, which is notable, but relatively small compared to the $250k cost of the battery system itself. Overall, it is clear that the total installed cost, and ongoing operational costs, of a solution must be considered when evaluating its feasibility.

Despite the savings potential from improving system control, the overall lifetime cost for installing a backup battery system remains relatively high. The nominal MPC scenario still results in an NPV of -$187k, which as discussed represents the lifetime cost of using a BESS system to provide backup power to the building. Typically this functionality would be provided by a diesel generator, which has an upfront cost of $60 - 75k with relatively low maintenance costs [43]. The poor lifetime performance for the BESS control scenarios is mostly due to the high upfront cost of a BESS system itself, estimated at around $333/kWh in this study. Sensitivity analysis shows that the BESS installation cost is a significant parameter, for example, reducing the total unit cost by 50% to $167/kWh would improve the NPV from -$187k to -$62k. This could be achievable in the coming decades, with lithium pack costs estimated to fall to around $100/kWh by 2035, and $71/kWh by 2050 [42]. Importantly these price forecasts only relate to the lithium packs themselves, so assuming the same ratio of pack cost to total installed cost used in this study (50%), this would give $200/kWh BESS cost by 2035 and $142/kWh by 2050.

Volatility in electricity prices is also a significant parameter that affects the performance of the MPC scenario. When considering the highly volatile electricity prices experienced during the Russian invasion of Ukraine, the net annual savings of the MPC scenario in year 1 increases by over 100%, from $10.7k to $22.8k. The battery is utilised more to provide load shifting, which slightly decreases its lifetime, but still improves the overall NPV from -$187k to -$99k. The generalisable MPC formulation is well able to adapt to the new electricity price profile without any modification to the formulation, which is a benefit compared to the rule-based control approaches in S1 and S2. Although it is unlikely electricity prices will return to these extreme levels for a sustained period, higher volatility in electricity prices could be experienced in the future. Renewable generation capacity is expected to grow across the world, along with increased electrification in areas like transport and heating. These factors will exacerbate the existing mismatch between electricity generation and demand, increasing price volatility across the day. In these cases, MPC approaches offer an attractive solution to reduce operating costs and robustly managing flexible energy systems.

6. Conclusions

Smart management of integrated energy systems is essential to support the ongoing decarbonisation of the built environment. There are many studies in this area, but few focus on the real-world implementation and lifetime cost of advanced control solutions. With this motivation, this paper simulates and compares the lifetime performance of two rule-based controllers and a supervisory MPC scheme to operate a commercial PV-battery system. By presenting this comprehensive financial analysis based on data from an existing site, our work supports the informed uptake of smart control schemes in the built environment.

The upfront cost of the battery is estimated at $250k, with an ongoing maintenance cost of $1.6k/yr. The existing rule-based controller saves 2.9% in annual operating costs compared to the baseline approach which doesn't use a battery system. These savings are increased to 4.3% by considering an informed rule-based controller which is configured using the existing hardware, but with informed knowledge of the PV and building loads, and typical electricity price dynamics. Then, a supervisory MPC approach is formulated to minimise the net cost of operating the site, taking into account time varying import costs as well as export earnings. Here, annual operating savings increase to 6%, taking into account the $13.7k cost to integrate the existing battery controller with the MPC scheme, and additional $4.3k/yr to run the cloud-based platform. In addition, annual carbon emissions are reduced by 9.8% despite not being explicitly considered, due to the correlation between high carbon intensity high energy prices. Further sensitivity analysis showed that MPC savings increase to 13.3% when considering volatile energy prices from 2022. Despite these control improvements, all control scenarios have a negative NPV, primarily due to the high upfront cost of battery systems.

CRediT authorship contribution statement

Max Bird: Writing – review & editing, Writing – original draft, Visualization, Validation, Software, Methodology, Investigation, Formal analysis, Data curation, Conceptualization. **Reewa Andraos:** Writing – original draft, Visualization, Software, Methodology, Investigation, Formal analysis, Data curation, Conceptualization. **Salvador Acha:** Writing – review & editing, Supervision, Resources, Project administration, Funding acquisition, Conceptualization. **Nilay Shah:** Writing – review & editing, Supervision, Resources, Funding acquisition.

Declaration of competing interest

The authors declare that they have no known competing financial interests or personal relationships that could have appeared to influence the work reported in this paper.

Acknowledgements

This research was supported by funds provided via the Imperial College London – Sainsbury's Supermarkets Ltd. Partnership.

Data availability

The authors do not have permission to share data.

References

[1] L. Bird, D. Lew, M. Milligan, E.M. Carlini, A. Estanqueiro, D. Flynn, E. Gomez-Lazaro, H. Holttinen, N. Menemenlis, A. Orths, P.B. Eriksen, J.C. Smith, L. Soder, P. Sorensen, A. Altiparmakis, Y. Yasuda, J. Miller, Wind and solar energy curtailment: a review of international experience, Renew. Sustain. Energy Rev. 65 (2016) 577–586, https://doi.org/10.1016/j.rser.2016.06.082, https://www.sciencedirect.com/science/article/pii/S1364032116303161.

[2] D. Newbery, National energy and climate plans for the island of Ireland: wind curtailment, interconnectors and storage, Energy Policy 158 (2021) 112513, https://doi.org/10.1016/j.enpol.2021.112513, https://www.sciencedirect.com/science/article/pii/S0301421521003839.

[3] O.H. Anuta, P. Taylor, D. Jones, T. McEntee, N. Wade, An international review of the implications of regulatory and electricity market structures on the emergence of grid scale electricity storage, Renew. Sustain. Energy Rev. 38 (2014) 489–508, https://doi.org/10.1016/j.rser.2014.06.006, https://www.sciencedirect.com/science/article/pii/S1364032114004432.

[4] J. Crawley, C. Johnson, P. Calver, M. Fell, Demand response beyond the numbers: a critical reappraisal of flexibility in two United Kingdom field trials, Energy Res. Soc. Sci. 75 (2021) 102032, https://doi.org/10.1016/j.erss.2021.102032, https://www.sciencedirect.com/science/article/pii/S2214629621001250.

[5] G. Dutta, K. Mitra, A literature review on dynamic pricing of electricity, J. Oper. Res. Soc. 68 (10) (2017) 1131–1145, https://doi.org/10.1057/s41274-016-0149-4.

[6] U. C. on Climate Change, The sixth carbon budget, https://www.theccc.org.uk/publication/sixth-carbon-budget/, December 2020.

[7] E. O'Dwyer, I. Pan, S. Acha, N. Shah, Smart energy systems for sustainable smart cities: current developments, trends and future directions, Appl. Energy 237 (2019) 581–597, https://doi.org/10.1016/j.apenergy.2019.01.024, https://www.sciencedirect.com/science/article/pii/S0306261919300248.

[8] A. Marvuglia, A. Messineo, G. Nicolosi, Coupling a neural network temperature predictor and a fuzzy logic controller to perform thermal comfort regulation in an office building, Build. Environ. 72 (2014) 287–299.

[9] J. Drgoňa, D. Picard, M. Kvasnica, L. Helsen, Approximate model predictive building control via machine learning, Appl. Energy 218 (2018) 199–216.

[10] P. Ferreira, A. Ruano, S. Silva, E. Conceicao, Neural networks based predictive control for thermal comfort and energy savings in public buildings, Energy Build. 55 (2012) 238–251.

[11] G.T. Costanzo, S. Iacovella, F. Ruelens, T. Leurs, B.J. Claessens, Experimental analysis of data-driven control for a building heating system, Sustain. Energy Grids Netw. 6 (2016) 81–90.

[12] P. Stoffel, L. Maier, A. Kümpel, T. Schreiber, D. Müller, Evaluation of advanced control strategies for building energy systems, Energy Build. 280 (2023) 112709, https://doi.org/10.1016/j.enbuild.2022.112709, https://www.sciencedirect.com/science/article/pii/S0378778822008805.

[13] J. Drgoňa, J. Arroyo, I. Cupeiro Figueroa, D. Blum, K. Arendt, D. Kim, E.P. Ollé, J. Oravec, M. Wetter, D.L. Vrabie, L. Helsen, All you need to know about model predictive control for buildings, Annu. Rev. Control 50 (2020) 190–232, https://doi.org/10.1016/j.arcontrol.2020.09.001, https://www.sciencedirect.com/science/article/pii/S1367578820300584.

[14] W. Yu, P. Patros, B. Young, E. Klinac, T.G. Walmsley, Energy digital twin technology for industrial energy management: classification, challenges and future, Renew. Sustain. Energy Rev. 161 (2022) 112407, https://doi.org/10.1016/j.rser.2022.112407, https://www.sciencedirect.com/science/article/pii/S136403212200315X.

[15] A. Kathirgamanathan, M. De Rosa, E. Mangina, D.P. Finn, Data-driven predictive control for unlocking building energy flexibility: a review, Renew. Sustain. Energy Rev. 135 (2021) 110120, https://doi.org/10.1016/j.rser.2020.110120, https://www.sciencedirect.com/science/article/pii/S1364032120304111.

[16] A.D. Georgakarakos, M. Mayfield, E.A. Hathway, Battery storage systems in smart grid optimised buildings, in: Annual Conference in Energy Storage and Its Applications, 3rd CDT-ESA-AC, in: Energy Procedia, vol. 151, 2018, pp. 23–30, 3rd, The University of Sheffield, UK, September 2018, pp. 11–12, https://www.sciencedirect.com/science/article/pii/S1876610218305630.

[17] G.P. Henze, C. Felsmann, G. Knabe, Evaluation of optimal control for active and passive building thermal storage, Int. J. Therm. Sci. 43 (2) (2004) 173–183, https://doi.org/10.1016/j.ijthermalsci.2003.06.001, https://www.sciencedirect.com/science/article/pii/S1290072903001327.

[18] G. Merei, J. Moshövel, D. Magnor, D.U. Sauer, Optimization of self-consumption and techno-economic analysis of pv-battery systems in commercial applications, Appl. Energy 168 (2016) 171–178, https://doi.org/10.1016/j.apenergy.2016.01.083, https://www.sciencedirect.com/science/article/pii/S0306261916300708.

[19] Z. Wang, M. Luther, P. Horan, J. Matthews, C. Liu, Technical and economic analyses of pv battery systems considering two different tariff policies, Sol. Energy 267 (2024) 112189, https://doi.org/10.1016/j.solener.2023.112189, https://www.sciencedirect.com/science/article/pii/S0038092X2300823X.

[20] Y. Zhang, A. Lundblad, P.E. Campana, F. Benavente, J. Yan, Battery sizing and rule-based operation of grid-connected photovoltaic-battery system: a case study in Sweden, Energy Convers. Manag. 133 (2017) 249–263, https://doi.org/10.1016/j.enconman.2016.11.060, https://www.sciencedirect.com/science/article/pii/S019689041631069X.

[21] J. Liu, X. Chen, H. Yang, Y. Li, Energy storage and management system design optimization for a photovoltaic integrated low-energy building, Energy 190 (2020) 116424, https://doi.org/10.1016/j.energy.2019.116424, https://www.sciencedirect.com/science/article/pii/S036054421932119X.

[22] R. Manojkumar, K.P. Inala, Optimised rule-based peak shaving and its impact on annual energy cost reduction, Int. J. Ambient Energy 45 (1) (2024) 2397672, https://doi.org/10.1080/01430750.2024.2397672.

[23] K. Zhang, A. Prakash, L. Paul, D. Blum, P. Alstone, J. Zoellick, R. Brown, M. Pritoni, Model predictive control for demand flexibility: real-world operation of a commercial building with photovoltaic and battery systems, Adv. Appl. Energy 7 (2022) 100099, https://doi.org/10.1016/j.adapen.2022.100099, https://www.sciencedirect.com/science/article/pii/S2666792422000178.

[24] M. Goldsworthy, T. Moore, M. Peristy, M. Grimeland, Cloud-based model-predictive-control of a battery storage system at a commercial site, Appl. Energy 327 (2022) 120038, https://doi.org/10.1016/j.apenergy.2022.120038, https://www.sciencedirect.com/science/article/pii/S0306261922012958.

[25] M. Alramlawi, A. Gabash, E. Mohagheghi, P. Li, Optimal operation of hybrid pv-battery system considering grid scheduled blackouts and battery lifetime, Sol. Energy 161 (2018) 125–137, https://doi.org/10.1016/j.solener.2017.12.022, https://www.sciencedirect.com/science/article/pii/S0038092X17311040.

[26] M. Bird, C. Daveau, E. O'Dwyer, S. Acha, N. Shah, Real-world implementation and cost of a cloud-based mpc retrofit for hvac control systems in commercial buildings, Energy Build. 270 (2022) 112269, https://doi.org/10.1016/j.enbuild.2022.112269, https://www.sciencedirect.com/science/article/pii/S0378778822004406.

[27] B. Xu, A. Oudalov, A. Ulbig, G. Andersson, D.S. Kirschen, Modeling of lithium-ion battery degradation for cell life assessment, IEEE Trans. Smart Grid 9 (2) (2018) 1131–1140, https://doi.org/10.1109/TSG.2016.2578950.

[28] J. Cai, H. Zhang, X. Jin, Aging-aware predictive control of pv-battery assets in buildings, Appl. Energy 236 (2019) 478–488, https://doi.org/10.1016/j.apenergy.2018.12.003, https://www.sciencedirect.com/science/article/pii/S0306261918318208.

[29] X. Jin, A. Vora, V. Hoshing, T. Saha, G. Shaver, R.E. García, O. Wasynczuk, S. Varigonda, Physically-based reduced-order capacity loss model for graphite anodes in li-ion battery cells, J. Power Sources 342 (2017) 750–761, https://doi.org/10.1016/j.jpowsour.2016.12.099, https://www.sciencedirect.com/science/article/pii/S037877531631802X.

[30] Eaton, Xstorage home warranty document, https://www.eaton.com/de/en-gb/catalog/energy-storage/xstorage-home.html#tab-3. (Accessed 2 June 2024).

[31] Eaton, Eaton xstorage compact technical datasheet, Tech. Rep., Eaton Corporation, 2024, https://www.eaton.com/content/dam/eaton/products/energy-storage/xstorage-compact/en-us/eaton-xstorage-compact-technical-datasheet-en-us.pdf. (Accessed 21 October 2024).

[32] NordPool, Day-ahead electricity prices, https://www.nordpoolgroup.com/en/. (Accessed 30 March 2024).

[33] S. Acha, G. Vieira, M. Bird, N. Shah, Modelling UK electricity regional costs for commercial buildings, Energy Build. 271 (2022) 112301, https://doi.org/10.1016/j.enbuild.2022.112301, https://www.sciencedirect.com/science/article/pii/S0378778822004728.

[34] N.G. Eso, Carbon intensity API, https://carbonintensity.org.uk/. (Accessed 20 May 2024).

[35] G. Mavromatidis, S. Acha, N. Shah, Diagnostic tools of energy performance for supermarkets using artificial neural network algorithms, Energy Build. 62 (2013) 304–314, https://doi.org/10.1016/j.enbuild.2013.03.020, https://www.sciencedirect.com/science/article/pii/S0378778813001886.

[36] B. Marion, B. Kroposki, K. Emery, J. del Cueto, D. Myers, C. Osterwald, Validation of a photovoltaic module energy ratings procedure at nrel, https://doi.org/10.2172/12187, 8 1999, https://www.osti.gov/biblio/12187.

[37] A. Mariaud, S. Acha, N. Ekins-Daukes, N. Shah, C.N. Markides, Integrated optimisation of photovoltaic and battery storage systems for UK commercial buildings, Appl. Energy 199 (2017) 466–478, https://doi.org/10.1016/j.apenergy.2017.04.067, https://www.sciencedirect.com/science/article/pii/S0306261917304646.

[38] K. Mongird, V. Viswanathan, P. Balducci, J. Alam, V. Fotedar, V. Koritarov, B. Hadjerioua, An evaluation of energy storage cost and performance characteristics, Energies 13 (13) (2020), https://doi.org/10.3390/en13133307, https://www.mdpi.com/1996-1073/13/13/3307.

[39] E. Stoikou, Lithium-ion battery pack prices hit record low of $139/kwh, bloombergNEF report on battery pack prices, https://about.bnef.com/blog/lithium-ion-battery-pack-prices-hit-record-low-of-139-kwh/, November 2023.

[40] OpenWeather, Irradiance forecasting tool, https://openweathermap.org/. (Accessed 14 May 2024).

[41] W. Liu, X. Zhang, L. Huang, H. Zhang, H. Yan, High-energy-density solid-state lithium batteries enabled by an ionic-liquid-based electrolyte: suppression of lithium dendrites and improvement of safety performance, Adv. Energy Mater. 11 (27) (2021) 2100771, https://doi.org/10.1002/aenm.202100771, https://onlinelibrary.wiley.com/doi/full/10.1002/aenm.202100771.

[42] L. Mauler, F. Duffner, W.G. Zeier, J. Leker, Battery cost forecasting: a review of methods and results with an outlook to 2050, Energy Environ. Sci. 14 (2021) 4712–4739, https://doi.org/10.1039/D1EE01530C.

[43] Y. Sawle, S. Gupta, A.K. Bohre, A novel methodology for scrutiny of autonomous hybrid renewable energy system, Int. J. Energy Res. 42 (2) (2018) 570–586, https://doi.org/10.1002/er.3841, https://onlinelibrary.wiley.com/doi/pdf/10.1002/er.3841, https://onlinelibrary.wiley.com/doi/abs/10.1002/er.3841.